Source decomposition of eddy-covariance CO2 flux measurements for evaluating a high-resolution urban CO2 emissions inventory

Kai Wu, Kenneth J. Davis, Natasha L. Miles, Scott J. Richardson, Thomas Lauvaux, Daniel P. Sarmiento, Nikolay V. Balashov, Klaus Keller, Jocelyn Turnbull, Kevin R. Gurney, et al.

ENVIRONMENTAL RESEARCH
LETTERS

LETTER • OPEN ACCESS

Source decomposition of eddy-covariance CO_2 flux measurements for evaluating a high-resolution urban CO_2 emissions inventory

To cite this article: Kai Wu *et al* 2022 *Environ. Res. Lett.* **17** 074035

ENVIRONMENTAL RESEARCH
LETTERS

LETTER

Source decomposition of eddy-covariance CO_2 flux measurements for evaluating a high-resolution urban CO_2 emissions inventory

Kai Wu[1,10,*], **Kenneth J Davis**[1,2], **Natasha L Miles**[1], **Scott J Richardson**[1], **Thomas Lauvaux**[3], **Daniel P Sarmiento**[4], **Nikolay V Balashov**[4], **Klaus Keller**[5], **Jocelyn Turnbull**[6,7], **Kevin R Gurney**[8,9], **Jianming Liang**[9] **and Geoffrey Roest**[8]

[1] Department of Meteorology and Atmospheric Science, The Pennsylvania State University, University Park, PA 16802, United States of America
[2] Earth and Environmental Systems Institute, The Pennsylvania State University, University Park, PA 16802, United States of America
[3] Laboratoire des Sciences du Climat et de l'Environnement, IPSL, CEA Saclay, 91191 Gif sur Yvette, Cedex, France
[4] NASA Goddard Space Flight Center, Greenbelt, MD 20771, United States of America
[5] Thayer School of Engineering, Dartmouth College, Hanover, NH 03755, United States of America
[6] Rafter Radiocarbon Laboratory, GNS Science, Lower Hutt 5040, New Zealand
[7] CIRES, University of Colorado at Boulder, Boulder, CO 80309, United States of America
[8] School of Informatics, Computing and Cyber Systems, Northern Arizona University, Flagstaff, AZ 85287, United States of America
[9] School of Life Sciences, Arizona State University, Tempe, AZ 85281, United States of America
[10] Now at: School of GeoSciences, The University of Edinburgh, Edinburgh, United Kingdom.
[*] Author to whom any correspondence should be addressed.

E-mail: kwu2@ed.ac.uk

OPEN ACCESS

RECEIVED
14 March 2022

REVISED
8 June 2022

ACCEPTED FOR PUBLICATION
27 June 2022

PUBLISHED
8 July 2022

Keywords: eddy-covariance flux measurements, source partitioning, emissions inventory, fossil fuel CO_2 emissions, biogenic CO_2 fluxes

Supplementary material for this article is available online

Abstract

We present the comparison of source-partitioned CO_2 flux measurements with a high-resolution urban CO_2 emissions inventory (Hestia). Tower-based measurements of CO and ^{14}C are used to partition net CO_2 flux measurements into fossil and biogenic components. A flux footprint model is used to quantify spatial variation in flux measurements. We compare the daily cycle and spatial structure of Hestia and eddy-covariance derived fossil fuel CO_2 emissions on a seasonal basis. Hestia inventory emissions exceed the eddy-covariance measured emissions by 0.36 μmol m^{-2} s^{-1} (3.2%) in the cold season and 0.62 μmol m^{-2} s^{-1} (9.1%) in the warm season. The daily cycle of fluxes in both products matches closely, with correlations in the hourly mean fluxes of 0.86 (cold season) and 0.93 (warm season). The spatially averaged fluxes also agree in each season and a persistent spatial pattern in the differences during both seasons that may suggest a bias related to residential heating emissions. In addition, in the cold season, the magnitudes of average daytime biological uptake and nighttime respiration at this flux site are approximately 15% and 27% of the mean fossil fuel CO_2 emissions over the same time period, contradicting common assumptions of no significant biological CO_2 exchange in northern cities during winter. This work demonstrates the effectiveness of using trace gas ratios to adapt eddy-covariance flux measurements in urban environments for disaggregating anthropogenic CO_2 emissions and urban ecosystem fluxes at high spatial and temporal resolution.

1. Introduction

Cities are becoming the focus for formulating and implementing carbon dioxide (CO_2) emissions mitigation efforts (Bulkeley 2013, Hutyra *et al* 2014, Lee and Koski 2014). Evaluating the effectiveness of emissions reduction efforts requires accurate CO_2 emissions estimates (Turnbull *et al* 2018, Lauvaux *et al* 2020). Although cities cover only 3% of the global land area, urban areas are home to 55% of the world's population, a proportion that is expected to increase to 68% by 2050 (Chaouad and Verzeroli 2018).

Overall, more than 70% of global fossil fuel CO_2 (CO_2ff) emissions are from urban areas (Edenhofer *et al* 2015). Efforts to assess and mitigate CO_2 emissions can provide benefits for urban sustainability and balanced economic growth (Hsu *et al* 2019).

Urban areas are consistently reported as a net source of CO_2 emissions (Velasco and Roth 2010). The eddy-covariance technique has been applied to measure urban CO_2 emissions in different cities for about two decades (Grimmond *et al* 2002, Nemitz *et al* 2002, Vogt *et al* 2006, Christen *et al* 2011, Järvi *et al* 2012, Christen 2014, Lietzke *et al* 2015, Ao *et al* 2016, Helfter *et al* 2016, Park and Schade 2016, Björkegren and Grimmond 2018). The attribution of urban CO_2 flux measurements is challenging due to the spatial heterogeneity, mixed emission sources and sinks, and limited spatial coverage of flux measurements (Aubinet *et al* 2012). Although most previous studies focus on the observed net CO_2 flux, a few studies attempt to partition flux measurements into fossil and biogenic components accounting for the temporal and spatial variability of the multiple sources and sinks. Menzer and McFadden (2017) modeled fossil CO_2 emissions based on winter data and extrapolated them to the growing season to estimate biogenic fluxes. Ishidoya *et al* (2020) demonstrated partitioning of CO_2 fluxes into liquid and gaseous fossil components using O_2 and CO_2 measurements. Sugawara *et al* (2021) used a nearby tower to estimate the biogenic component of a total CO_2 flux measurement.

Quantification of anthropogenic CO_2 emissions is challenging due to the difficulty of separating CO_2ff emissions from biogenic CO_2 (CO_2bio) fluxes (Basu *et al* 2020, Miller *et al* 2020). Previous studies demonstrated the feasibility of using ^{14}C isotope measurements to separate CO_2ff from CO_2bio fluxes (Miller *et al* 2012, Turnbull *et al* 2015, Basu *et al* 2016), but flask measurements of ^{14}C are expensive and discontinuous. Continuous measurements of carbon monoxide (CO) provide another approach to track CO_2ff emissions (Levin and Karstens 2007, Vogel *et al* 2010, Turnbull *et al* 2011, Silva *et al* 2013, Park and Schade 2016). Uncertainties in the CO to CO_2ff ratio, which vary as a function of emission sectors, complicate the attribution of urban CO_2 fluxes. The use of ^{14}C measurements to determine the ratio of CO to CO_2ff has not yet been applied to eddy covariance flux measurements. We attempt to combine the complementary strengths of CO and ^{14}C to decompose net CO_2 flux measurements, and use the partitioned CO_2ff emissions to evaluate a high-resolution emissions inventory.

Emissions inventories use activity data to aggregate urban CO_2ff emissions (Boden *et al* 2009, Gurney *et al* 2009, Olivier and Janssens-Maenhout 2012), but the differences among inventories are sizeable (Gately and Hutyra 2017, Oda *et al* 2019, Gurney *et al* 2020). Atmospheric inversions use inventories as prior estimates of emissions and optimize the emissions using atmospheric CO_2 mole fraction observations (Bréon *et al* 2015, Lauvaux *et al* 2016, 2020, Staufer *et al* 2016, Turner *et al* 2016, Kunik *et al* 2019). Two substantial sources of uncertainty in inverse estimates of urban CO_2ff emissions are uncertain CO_2bio fluxes and unknown error characteristics in emissions inventories (Wu *et al* 2018). The Hestia emissions inventory (Gurney *et al* 2012) was developed in part to support the Indianapolis Flux Experiment (INFLUX) and uses energy consumption, population density, and traffic data to quantify CO_2ff emissions for an entire urban landscape at an approximately 200 m and hourly resolution. While excellent agreement between Hestia and atmospheric inversions has been shown over multiple years at the scale of an entire city (Lauvaux *et al* 2020), the high-resolution performance of the Hestia inventory has not yet been evaluated with eddy-covariance flux measurements.

This study compares source-partitioned CO_2 eddy-covariance flux measurements with a high-resolution emissions inventory (Hestia) in a suburban region of Indianapolis, Indiana, USA. We partition the net CO_2 flux measurements into CO_2ff and CO_2bio components using a flux-gradient relationship (Stull 2012) and atmospheric CO measurements. ^{14}C isotope measurements are used to estimate the CO to CO_2ff ratio and reduce the uncertainty in the flux decomposition. The source decomposition methods are similar to those used by Ishidoya *et al* (2020) and Sugawara *et al* (2021). In addition, we use a flux footprint model (Kljun *et al* 2004, 2015) to match each flux measurement in space and time with the Hestia inventory to provide a direct comparison of independent estimates of anthropogenic CO_2 emissions at high spatial and temporal resolution. This is, to our knowledge, the first such comparison of these innovative and independent assessments of high-resolution urban CO_2 emissions, and is timely given the growing interest in monitoring the impact of urban systems on atmospheric composition.

2. Data and methods

2.1. Site descriptions and atmospheric CO_2 flux measurements

The INFLUX observation network (Davis *et al* 2017) measures atmospheric CO_2 and CO mole fractions, and net CO_2 fluxes in and around Indianapolis, IN (figure 1). The locations, sampling heights and measurements at these sites are described by Miles *et al* (2017) and the instrument performance is described by Richardson *et al* (2017). ^{14}C isotope measurements, collected weekly, are used to evaluate CO to CO_2ff ratios using methods described by Turnbull *et al* (2015).

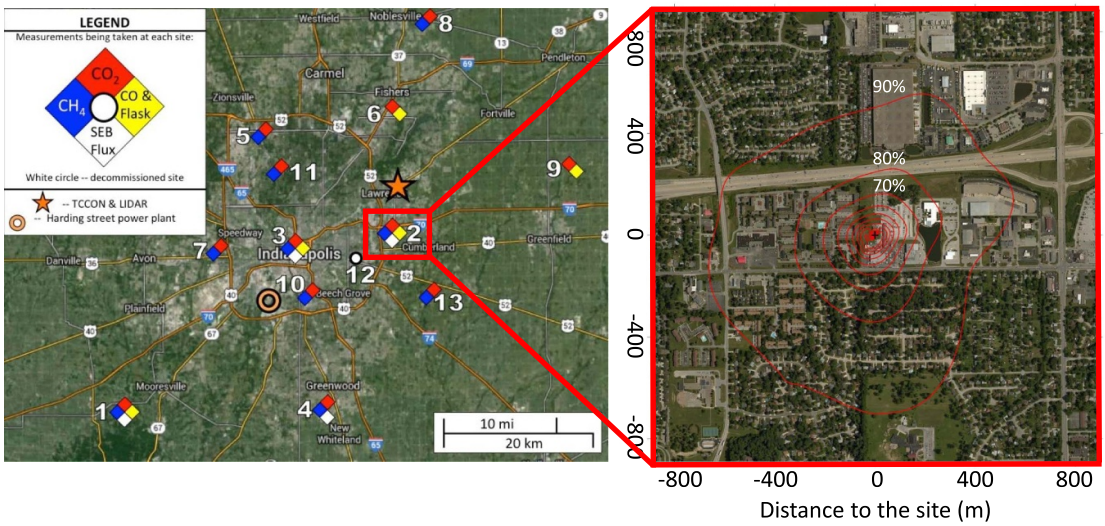

Figure 1. The INFLUX measurement network in Indianapolis, IN (left) and cumulative flux footprints from January through July in 2013 at Tower 2 (right). The contours in the right panel represent the percentage of the time-integrated flux that comes from within that boundary (the base map is from Google Maps, Imagery © 2019 Google, Map data © 2019). The color of the marker in the left panel represents the measurements at each site: red for CO_2, yellow for CO and ^{14}C, blue for CH_4, and white for surface energy balance fluxes. The coordinates in the right panel are the distance (m) to the measurement site.

Since the flux decomposition requires atmospheric measurements of CO_2 and CO mole fractions at different heights as well as ^{14}C isotope measurements, the need for multiple observational datasets limits the time and location for which we have available data. In total, there are seven months (January through July, 2013) that include all of these data sets (atmospheric measurements of CO_2 and CO mole fractions, ^{14}C isotope, and CO_2 flux) available at Tower 2 (39.7978° N, 86.0183° W), which is located in a heterogeneous suburban environment (figures 1 and S1). There is a highway to the north, urban vegetation to the south, and neighborhoods with detached houses. The heterogeneous surroundings present a good test of our ability to partition net CO_2 flux measurements into fossil and biogenic components and to use flux footprint analyses to compare the spatial and temporal heterogeneity of source-specific flux data and the Hestia inventory.

The flux instrumentation, which includes a sonic anemometer (Campbell Scientific, CSAT-3) and a high-frequency open-path infrared CO_2 sensor (LI-COR Environmental, LI-7500), is mounted at 30 m above ground level (AGL) on Tower 2. The eddy-covariance technique measures the covariance between fluctuations in vertical wind velocity and CO_2 density to detect the integrated exchange of CO_2 between land and atmosphere (Lee *et al* 2004, Foken and Napo 2008, Aubinet *et al* 2012). We use flux calculation and filtering methods recommended by Vickers and Mahrt (1997). We filter out extreme values outside 3.5 σ range of the data (0.2% of data are filtered out) and nighttime fluxes during weak turbulence conditions when the friction velocity is less than 0.2 m s^{-1} (3.6% of data are filtered out) (Gu *et al* 2005). Negative fluxes show contributions of photosynthesis to the flux data (figure S2). Based on the similarity of the diurnal variation of net CO_2 flux measurements (figure S3), we define the cold season as January–March (JFM) and the warm season as April–July (AMJJ).

2.2. Partitioning fossil and biogenic CO_2 fluxes

To partition fossil and biogenic components from the net CO_2 flux measurements, we apply a flux-gradient method and atmospheric CO measurements. In addition to flux measurements, we also measure CO_2 and CO mole fractions at 10 and 40 m heights AGL at Tower 2 (Miles *et al* 2017). We use the net flux measurement (F_{CO_2}) and vertical gradient in CO_2 mole fraction (∇C_{CO_2}) to solve for the eddy diffusivity (K):

$$K = -\frac{F_{CO_2}}{\nabla C_{CO_2}}, \tag{1}$$

and use that eddy diffusivity and the CO vertical gradient (∇C_{CO}) to solve for the CO flux (F_{CO}):

$$F_{CO} = -K \nabla C_{CO}. \tag{2}$$

The fossil fuel CO_2 emission (F_{CO_2ff}) is estimated by combining the CO flux with the emission ratio (R) of CO to CO_2ff:

$$F_{CO_2ff} = \frac{F_{CO}}{R}, \tag{3}$$

and we attribute the difference between the net flux measurement and the partitioned fossil fuel CO_2 emission to the biogenic CO_2 flux (F_{CO_2bio}):

$$F_{CO_2bio} = F_{CO_2} - F_{CO_2ff}. \tag{4}$$

There are three assumptions in this method: (a) turbulent eddies are small enough that local scalar gradients are proportional to turbulent fluxes; (b) CO and CO_2 are subject to the same vertical mixing processes; (c) within the turbulent flux footprint, CO is mainly produced by fossil fuel combustion simultaneously with CO_2ff emissions. We filter out counter-gradient fluxes, and limit the eddy diffusivity and CO flux within 3.5 σ range of their estimates to screen out extreme values caused by tiny denominators. Human respiration, which would appear in this decomposition as a biological flux, is estimated based on the population density of Indianapolis (896 people km^{-2} in the year 2013) multiplied by a typical emission rate of 942 gCO_2 $person^{-1}$ day^{-1} (Prairie and Duarte 2007).

The emission ratio of CO to CO_2ff is estimated from flask measurements of ^{14}C and CO measurements (Turnbull *et al* 2015). The urban CO and ^{14}C enhancements are estimated by the differences between Tower 2 and upwind background sites (Tower 1 or 9 depending on the wind direction). The median and mean values of CO to CO_2ff ratios estimated from these enhancements are 9.52 and 8.98 ppb ppm^{-1} (cold season) and 9.13 and 9.02 ppb ppm^{-1} (warm season) (figure S4). We use 9 ppb ppm^{-1} as an approximate value to infer CO_2ff emissions. To test the uncertainty of using different ratios on the flux decomposition, we vary the emission ratio to 11 and 7 (9 ± 2) ppb ppm^{-1}. These are plausible bounds (table 2 in Turnbull *et al* 2015) for this flux site, representing approximately the 70th and 30th percentiles of the values. With a linear relation of the flux decomposition to the emission ratio (equation (3)), this maximum and minimum boundary approach represents our limited confidence in the emission ratio and its uncertainty bounds. A more formal error propagation would suggest more confidence than we have in our estimate of the uncertainty in the emission ratio. In addition, since traffic emissions are likely to have a higher ratio and residential emissions have a smaller ratio, we add another scenario with a CO to CO_2ff ratio of 15 ppb ppm^{-1} for northerly winds from the highway and 7 ppb ppm^{-1} for the other wind directions based on sectoral emission ratios estimated by Turnbull *et al* (2015).

2.3. Flux footprint and emissions inventory

A flux footprint, which is defined as the contributing area upwind from the measurement site (Leclerc and Foken 2014), is essential to account for the spatial heterogeneity of emission sources. We use a two-dimensional flux footprint model (https://footprint.kljun.net/) (Kljun *et al* 2004, 2015) to match with the Hestia inventory and estimate the emissions predicted by the inventory at the tower location. Flux footprints were computed with a spatial resolution of approximately 2 m. The size of footprint depends on measurement height, surface roughness, and atmospheric thermal stability. The footprint will increase with an increase in measurement height, with a decrease in surface roughness, and with an increase in atmospheric thermal stability (Burba and Anderson 2010). Tower-based measurements of wind field and boundary layer characteristics are used to estimate the input parameters of the flux footprint model (measurement height above displacement height, roughness length, Obukhov length, friction velocity, mean wind speed, boundary layer height, standard deviation (SD) of lateral velocity fluctuations). The displacement height and roughness length are estimated as 6 and 0.45 m, respectively. The displacement height is estimated to be 0.7 times the local mean building and tree heights (Weng *et al* 2013) and the roughness length is computed from the mean wind and momentum fluxes measured at 30 m AGL (Drew *et al* 2013, Kent *et al* 2017). We estimate the flux footprint (f) for each hourly flux measurement. After interpolating the Hestia inventory to the coordinates of each flux footprint, we weight the hourly Hestia emissions (Q_H) with the spatially-resolved fractional flux contributions (f) at the same time and sum over the domain of flux footprint (R) to produce a spatially-weighted estimate of the Hestia flux that would be measured at the tower (F_H):

$$F_H = \sum_{i=1}^{R} Q_H(x_i, y_i) f(x_i, y_i) \delta x \delta y. \quad (5)$$

The emissions predicted by the Hestia inventory at the tower (F_H) are compared with the partitioned CO_2ff flux measurements (F_{CO_2ff} in equation (3)).

3. Results

Net CO_2 flux measurements, decomposed as a function of time and space, behave as expected given the environment surrounding the tower. Observed CO_2 emissions are larger in the cold season than the warm season (figure 2(a)), perhaps due to increased emissions from building heating around the tower (figures 1 and S1). In the cold season, there are two prominent peaks in emissions likely corresponding to peaks in traffic volume during rush hours. In the warm season, CO_2ff emissions are mixed with photosynthesis and respiration from urban vegetation within the flux footprints. The daytime photosynthetic uptake of CO_2 indicates the role of urban vegetation. The data show high emissions from the north, and lower emissions or net uptake from the south (figures 2(b) and (c)), consistent with the highway to the north and urban vegetation to the south of the tower.

Partitioning of the net observed CO_2 fluxes into fossil and biogenic components yields plausible temporal behavior of these flux components (figure 3). While smaller than the estimated CO_2ff emissions,

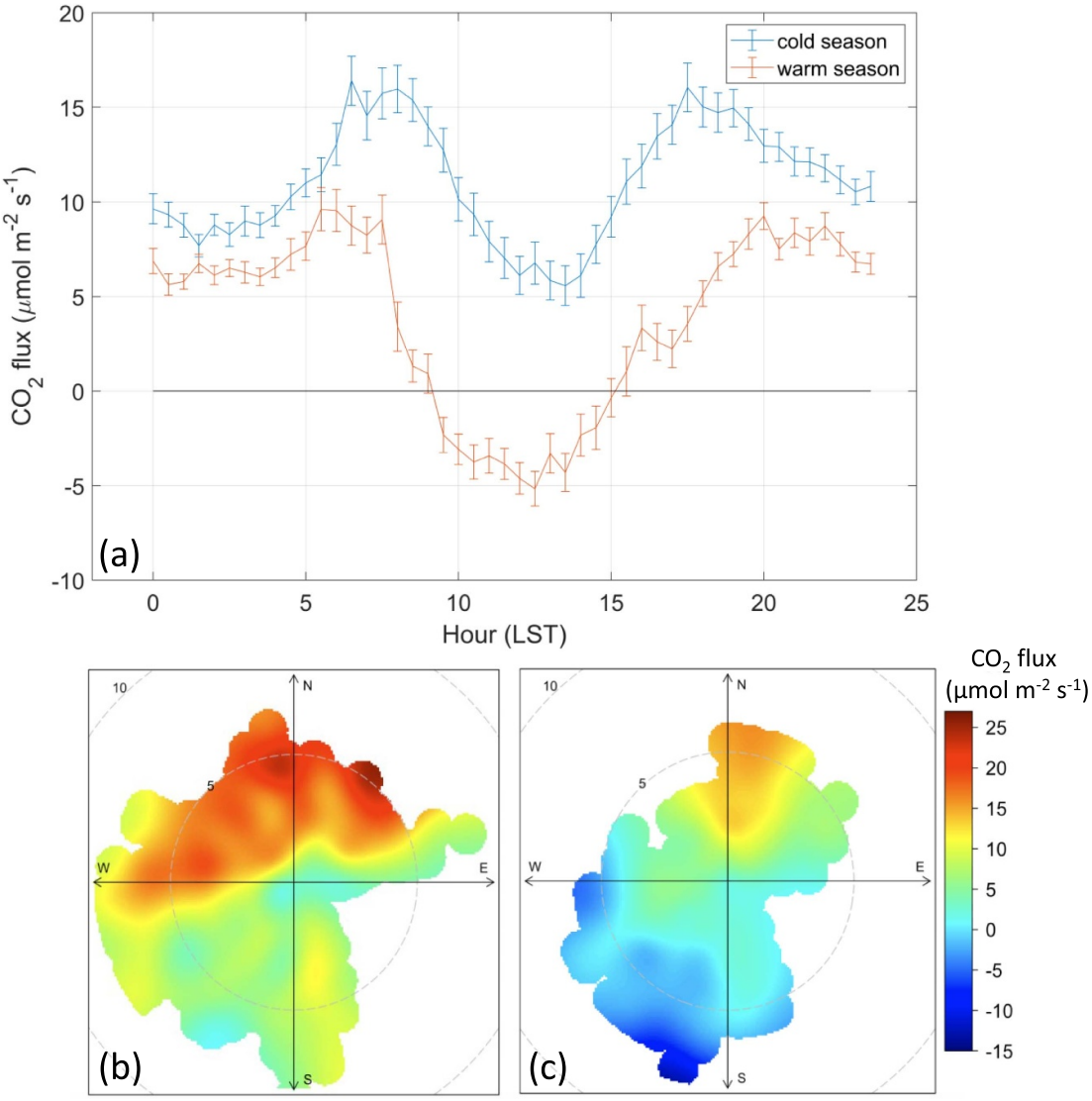

Figure 2. Diurnal variation of seasonally-averaged CO_2 flux measurements during the cold (JFM) and warm (AMJJ) seasons in 2013 (a). Error bars indicate the standard errors of the seasonal means. Spatial variation of time-averaged CO_2 fluxes in the cold (b) and warm (c) seasons. Color indicates flux magnitude. The radial coordinate corresponds to wind speed ($m\,s^{-1}$) and the angular coordinate is the wind direction.

the magnitude of the cold season daytime (9 to 20 LST) averaged biological uptake is 15% of the mean CO_2ff emissions over the same time period and the ecosystem respiration averaged over nighttime (21 to 8 LST) is 27% of the mean nighttime CO_2ff emissions. These are non-negligible flux magnitudes that need to be considered to obtain accurate CO_2ff emissions (figure 3(a)). Human respiration is estimated to be 0.22 $\mu mol\,m^{-2}\,s^{-1}$, which would contribute about 10% of the average nighttime CO_2bio fluxes in the cold season. A typical pattern of ecosystem fluxes emerges in the warm season (figure 3(b)). The warm season CO_2bio fluxes are equal in amplitude to the CO_2ff emissions, emphasizing the importance of accounting for CO_2bio fluxes in attempts to quantify urban CO_2ff emissions. The error bars are the standard errors of the seasonal means, which represent a mixture of day-to-day variability, random measurement errors, and uncertainty in the flux decomposition using a typical emission ratio (9 ppb ppm^{-1}). We will examine the impacts of using different ratios on the flux decomposition.

The seasonally-averaged partitioned CO_2ff emissions estimates show remarkable similarity to the Hestia inventory when matched in space and time using the flux footprint model. Seasonal-mean CO_2ff emissions differ (Hestia minus observed CO_2ff emissions) by 0.36 $\mu mol\,m^{-2}\,s^{-1}$ (3.2% of the mean partitioned CO_2ff emissions) in the cold season (figure 4(a)) and 0.62 $\mu mol\,m^{-2}\,s^{-1}$ (9.1% of the mean partitioned CO_2ff emissions) in the warm season (figure 4(b)). The corresponding SDs of the residuals are 8.91 and 7.52 $\mu mol\,m^{-2}\,s^{-1}$, which include random errors in the flux measurements. The temporal patterns of seasonally-averaged Hestia and the partitioned CO_2ff emissions also agree remarkably well (figures 4(c) and (d)). The correlation coefficients of the diurnal variations are 0.86

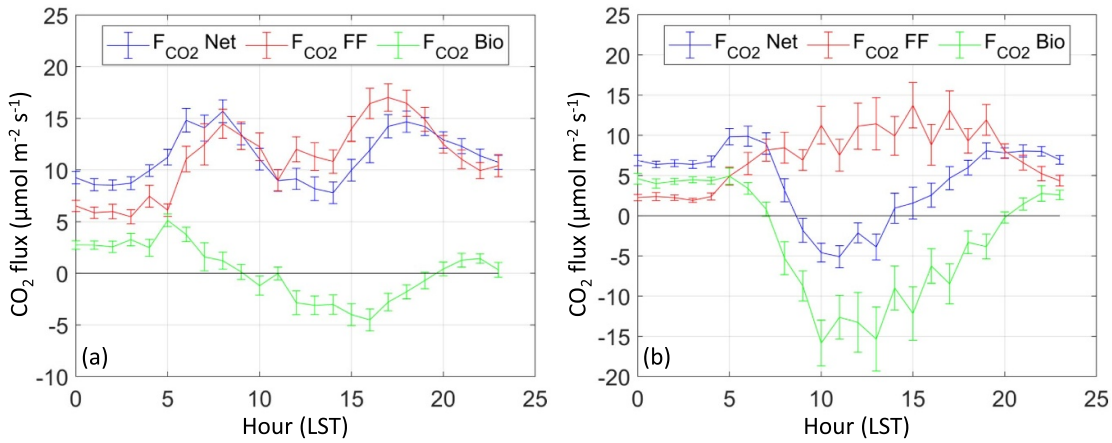

Figure 3. Diurnal variation of seasonally-averaged CO_2 flux measurements (F_{CO_2}Net) and the partitioned fossil fuel (F_{CO_2}FF) and biogenic (F_{CO_2}Bio) fluxes in the cold (JFM) (a) and warm (AMJJ) (b) seasons in 2013. Error bars are the standard errors of the seasonal means.

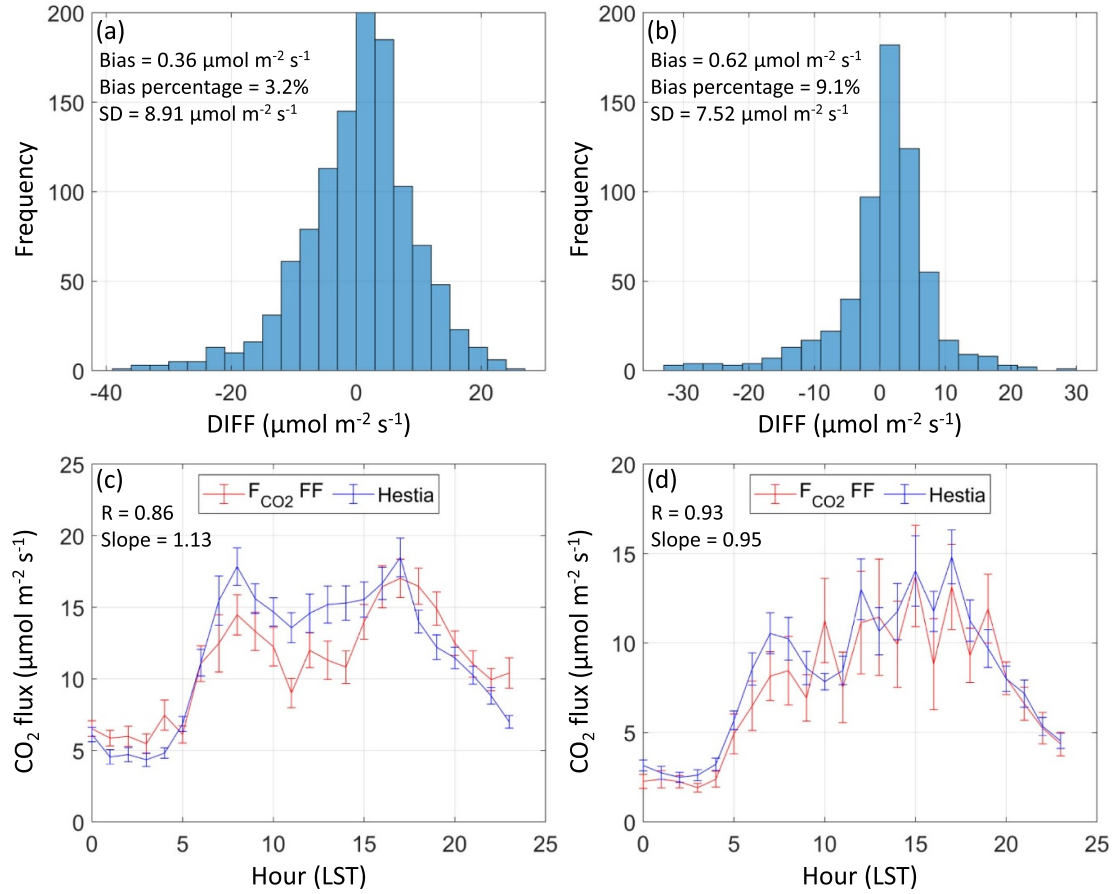

Figure 4. Histogram of flux differences between the Hestia inventory and the partitioned fossil fuel CO_2 emissions (Hestia minus observed CO_2ff emissions) in the cold (JFM) (a) and warm (AMJJ) (b) seasons in 2013. Bias, bias percentage compared to the mean partitioned CO_2ff emissions, and standard deviation (SD) of residuals are listed. Diurnal variation of seasonally-averaged CO_2ff emissions in the cold (c) and warm (d) seasons. Error bars are the standard errors of the seasonal means.

(cold season) and 0.93 (warm season), and the slopes are 1.13 and 0.95, respectively. The Hestia emissions are smaller during the night and higher during the day compared to the partitioned observations in the cold season (figures 4(c) and S5(a)), and consistently slightly higher than the partitioned observations in the warm season (figures 4(d) and S5(b)).

We also find similarity in the comparison of eddy-covariance and Hestia CO_2ff emissions as a function of wind direction (figure 5). In the cold season, the

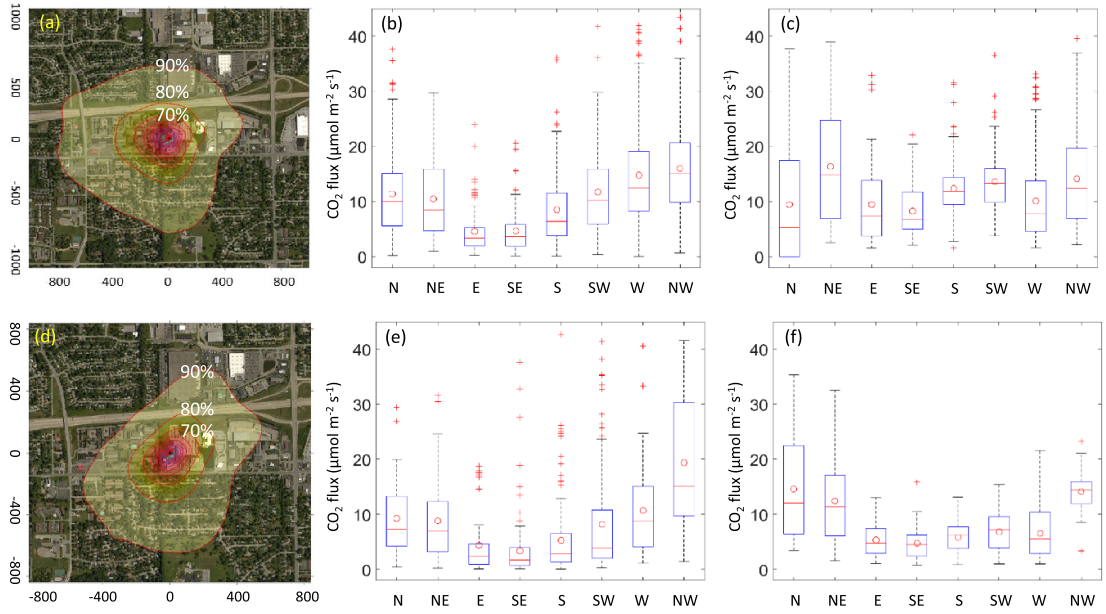

Figure 5. Cumulative flux footprints (a and d), the partitioned fossil fuel CO_2 emissions (b and e) and the Hestia inventory (c and f) for different wind directions. Panels a to c are in the cold season (JFM) and panels d to f are in the warm season (AMJJ) in 2013. The coordinates in the left panel indicate the distance (m) to the measurement site (the base map is from Google Maps, Imagery © 2019 Google, Map data © 2019). The contours represent the percentage of the time-integrated flux that comes from within that boundary and each contour represents a 10% interval. In the middle and right panels, the red circles, the lines and the plus marks represent the mean, the median and the outliers, respectively. The bottom and top edges of the box indicate the 25th and 75th percentiles. The whiskers extend to the most extreme data points not considered outliers that are defined as more than 1.5 times the interquartile range away from the top or bottom of the box.

Table 1. Statistics of flux differences (μmol m^{-2} s^{-1}) between the Hestia inventory and the partitioned fossil fuel CO_2 emissions (Hestia minus observed CO_2ff emissions) for different wind directions.

	DIFF	N	NE	E	SE	S	SW	W	NW
Cold	Median	−2.00	3.32	2.88	3.45	4.14	3.15	−4.47	−2.14
season	Mean	−1.93	5.88	4.88	3.58	3.84	1.89	−4.72	−1.87
(JFM)	RMSE[a]	10.98	9.27	8.22	5.63	7.45	8.00	10.40	9.06
Warm	Median	2.49	3.34	1.92	1.98	0.98	0.42	−2.71	−4.27
season	Mean	5.31	3.61	0.92	1.37	0.52	−1.32	−4.17	−5.21
(AMJJ)	RMSE	8.24	9.32	5.19	5.54	5.97	8.62	8.47	13.66

[a] Root mean square error.

Hestia emissions are higher than the observed CO_2ff emissions for all wind directions except the north, west and northwest wind (table 1). A similar pattern exists in the warm season. Since residential buildings lie upwind in the west and northwest wind directions (figures 1 and S1), we infer residential emissions could be the source of this discrepancy.

These results are somewhat sensitive to the choice of CO to CO_2ff ratio in the flux decomposition. Seasonal-mean flux bias and bias percentage change significantly when the emission ratio varies from 9 ppb ppm^{-1} to 11 or 7 ppb ppm^{-1} (figure S6 and table S1). Figure S6 shows the impact of plausible ratios on the diurnal cycle of the partitioned CO_2ff and CO_2bio fluxes. The lower bound of 7 ppb ppm^{-1} increases the CO_2ff emissions estimate (figure S6(b) and equation (3)), thus driving the CO_2bio fluxes down about 3 μmol m^{-2} s^{-1} in the cold season (figure S6(c) and equation (4)). This would strengthen the finding of daytime photosynthesis. The upper bound ratio of 11 ppb ppm^{-1} would increase CO_2bio fluxes by about 2 μmol m^{-2} s^{-1} in the cold season, leaving midday fluxes slightly negative and nighttime respiration at about 4 μmol m^{-2} s^{-1}. Similar results are shown in the warm season (figures S6(e) and S6(f)). The magnitude of the partitioned fluxes varies linearly with the change of emission ratio, but the diurnal cycle is not sensitive to this choice. The scenario with the space-varying emission ratio (15 and 7 ppb ppm^{-1}), which may be more realistic than a constant ratio, does not significantly change either the diurnal variation (figure S6) or the bias estimation (table S1) when compared to the default scenario (9 ppb ppm^{-1}).

4. Conclusions and discussion

The remarkable agreement between the Hestia inventory and the partitioned flux measurements suggests that both methods are able to describe the temporal and spatial variability in urban CO_2ff emissions at neighborhood scale. Neither approach has yet been cross-validated at such a high spatial and temporal resolution. The flux measurement partitioning is sensitive to the CO to CO_2ff emission ratio, but the consistency of Hestia and flux data suggests that flask measurements have accurately quantified that ratio. The success of this test suggests that these eddy-covariance flux decomposition methods can be used to quantify source-specific, neighborhood-scale CO_2ff emissions. Further the successful comparison to Hestia suggests that the algorithms and input data used in the inventory system are accurate and precise even at the fine resolution of the eddy-covariance flux measurements.

This study also shows the promise of using this approach for studying urban ecosystem CO_2 fluxes. Previous work has suggested that the edges found in urban ecosystems lead to fundamentally different behavior of these ecosystems (Reinmann *et al* 2020). These findings are largely based on chamber-scale flux measurements. It is not clear whether or not, when upscaled to spatial domains that integrate across many edges such as a suburban forest, existing ecosystem models and model parameters will suffice in describing urban CO_2bio fluxes. Current ecosystem models used in urban studies are largely devoid of urban ecosystem flux measurements in either calibration or evaluation due to lack of data (Hardiman *et al* 2017, Wu *et al* 2021). We suggest that the decomposition methods can serve as a new approach for obtaining ecosystem flux data necessary to develop the next generation of urban ecosystem models.

Finally, this study emphasizes the importance of urban ecosystem fluxes, both in the warm (growing) season and the cold (dormant) season. Our results appear to contradict the findings of Turnbull *et al* (2015) who found no net impact of biological CO_2 fluxes on CO_2 enhancements in Indianapolis outside of the growing season. We found the percentage of daytime biological uptake in the cold season is 15% compared to the mean CO_2ff emissions. Our results are consistent with the flask measurements (figure 5 in Turnbull *et al* 2015) which showed that, for Tower 2, the total CO_2 enhancement in the winter months was 0.8 to 0.9 times the CO_2ff enhancement, suggesting modest net biological uptake of CO_2 during these months within the city. The flask ^{14}C-based CO_2bio enhancement at Tower 2 averaged over the cold season for the three months of this study is −0.37 ppm (table S2) that is about 10% of the estimated fossil CO_2 enhancement (3.6 ppm), consistent with our eddy-covariance flux measurements. Turnbull *et al* (2015) found no net biological CO_2 contribution to the wintertime enhancements when averaging together four towers including Tower 2. The other towers likely have less influence from urban vegetation based on their position around the city. The importance of growing season biological fluxes has been shown in multiple observational (Turnbull *et al* 2015, Miller *et al* 2020) and inversion (Sargent *et al* 2018, Wu *et al* 2018, Lauvaux *et al* 2020) studies. Uncertainty in biological fluxes has a large impact on inverse flux estimates (Wu *et al* 2018, Lauvaux *et al* 2020). This flux decomposition approach enables evaluation of the modeled ecosystem flux priors using direct urban ecosystem CO_2 flux measurements. Further, a number of studies (Lauvaux *et al* 2016, Heimburger *et al* 2017) have made the reasonable assumption of neglecting CO_2bio fluxes in the dormant season. This work shows that urban ecosystems in Indianapolis are moderately active even in the cold season. Additional eddy-covariance flux measurements are needed to study the spatial and temporal variations in urban ecosystem CO_2 fluxes.

Data availability statement

The Hestia emission inventory is available at http://dx.doi.org/10.18434/T4/1503341. The eddy-covariance flux measurements and flask data are available at https://sites.psu.edu/influx/data. The CO_2 and CO mole fraction measurements are available at http://dx.doi.org/10.18113/D37G6P.

Acknowledgments

The authors thank Bernd J Haupt (PSU) for data acquisition and quality control. This work was funded by the National Institute of Standards and Technology (Project 70NANB10H245). T Lauvaux was supported by the French research program Make Our Planet Great Again (Project CIUDAD). K R Gurney, J Liang, and G Roest received support from the National Aeronautics and Space Administration (Grant NNX14AJ20G) and the National Institute of Standards and Technology (Grant 70NANB16H264N).

Conflict of interest

The authors declare no competing interests.

ORCID iDs

Kai Wu https://orcid.org/0000-0003-2054-4278
Kenneth J Davis https://orcid.org/0000-0002-1992-8381
Klaus Keller https://orcid.org/0000-0002-5451-8687

References

Ao X, Grimmond C, Chang Y, Liu D, Tang Y, Hu P, Wang Y, Zou J and Tan J 2016 Heat, water and carbon exchanges in the tall megacity of Shanghai: challenges and results *Int. J. Climatol.* **36** 4608–24

Aubinet M, Vesala T and Papale D 2012 *Eddy Covariance: A Practical Guide to Measurement and Data Analysis* (Dordrecht: Springer Science & Business Media)

Basu S, Lehman S J, Miller J B, Andrews A E, Sweeney C, Gurney K R, Xu X, Southon J and Tans P P 2020 Estimating US fossil fuel CO_2 emissions from measurements of ^{14}C in atmospheric CO_2 *Proc. Natl Acad. Sci.* **117** 13300–7

Basu S, Miller J B and Lehman S 2016 Separation of biospheric and fossil fuel fluxes of CO_2 by atmospheric inversion of CO_2 and $^{14}CO_2$ measurements: observation system simulations *Atmos. Chem. Phys.* **16** 5665–83

Björkegren A and Grimmond C 2018 Net carbon dioxide emissions from central London *Urban Clim.* **23** 131–58

Boden T A, Marland G and Andres R J 2009 *Global, Regional, and National Fossil-Fuel CO_2 Emissions* (Oak Ridge, TN: Carbon Dioxide Information Analysis Center, Oak Ridge National Laboratory, US Department of Energy) vol 10

Bréon F *et al* 2015 An attempt at estimating Paris area CO_2 emissions from atmospheric concentration measurements *Atmos. Chem. Phys.* **15** 1707–24

Bulkeley H 2013 *Cities and Climate Change* (London: Routledge)

Burba G and Anderson D 2010 *A Brief Practical Guide to Eddy Covariance Flux Measurements: Principles and Workflow Examples for Scientific and Industrial Applications* (Lincoln: Li-Cor Biosciences)

Chaouad R and Verzeroli M 2018 The urbanization of the world: facts and challenges *Rev. Int. Strategique* **112** 47–65

Christen A 2014 Atmospheric measurement techniques to quantify greenhouse gas emissions from cities *Urban Clim.* **10** 241–60

Christen A, Coops N, Crawford B, Kellett R, Liss K, Olchovski I, Tooke T, Van Der Laan M and Voogt J 2011 Validation of modeled carbon-dioxide emissions from an urban neighborhood with direct eddy-covariance measurements *Atmos. Environ.* **45** 6057–69

Davis K J *et al* 2017 The Indianapolis Flux Experiment (INFLUX): a test-bed for developing urban greenhouse gas emission measurements *Elementa* **5** 21

Drew D R, Barlow J F and Lane S E 2013 Observations of wind speed profiles over Greater London, UK, using a Doppler lidar *J. Wind Eng. Ind. Aerodyn.* **121** 98–105

Edenhofer O *et al* 2015 *Climate Change 2014: Mitigation of Climate Change* vol 3 (Cambridge: Cambridge University Press)

Foken T and Napo C J 2008 *Micrometeorology* (Berlin: Springer)

Gately C and Hutyra L 2017 Large uncertainties in urban-scale carbon emissions *J. Geophys. Res.* **122** 11242–60

Grimmond C, King T, Cropley F, Nowak D and Souch C 2002 Local-scale fluxes of carbon dioxide in urban environments: methodological challenges and results from Chicago *Environ. Pollut.* **116** S243–54

Gu L *et al* 2005 Objective threshold determination for nighttime eddy flux filtering *Agric. Forest Meteorol.* **128** 179–97

Gurney K R *et al* 2009 High resolution fossil fuel combustion CO_2 emission fluxes for the United States *Environ. Sci. Technol.* **43** 5535–41

Gurney K R, Liang J, Patarasuk R, Song Y, Huang J and Roest G 2020 The Vulcan version 3.0 high-resolution fossil fuel CO_2 emissions for the United States *J. Geophys. Res.* **125** e2020JD032974

Gurney K R, Razlivanov I, Song Y, Zhou Y, Benes B and Abdul-Massih M 2012 Quantification of fossil fuel CO_2 emissions on the building/street scale for a large US city *Environ. Sci. Technol.* **46** 12194–202

Hardiman B S, Wang J A, Hutyra L R, Gately, C K, Getson J M and Friedl M A 2017 Accounting for urban biogenic fluxes in regional carbon budgets *Sci. Total Environ.* **592** 366–72

Heimburger A M *et al* 2017 Assessing the optimized precision of the aircraft mass balance method for measurement of urban greenhouse gas emission rates through averaging *Elementa* **5** 26

Helfter C, Tremper A H, Halios C H, Kotthaus S, Bjorkegren A, Grimmond C S B, Barlow J F and Nemitz E 2016 Spatial and temporal variability of urban fluxes of methane, carbon monoxide and carbon dioxide above London, UK *Atmos. Chem. Phys.* **16** 10543–57

Hsu A *et al* 2019 A research roadmap for quantifying non-state and subnational climate mitigation action *Nat. Clim. Change* **9** 11–17

Hutyra L R, Duren R, Gurney K R, Grimm N, Kort, E A, Larson E and Shrestha G 2014 Urbanization and the carbon cycle: current capabilities and research outlook from the natural sciences perspective *Earth's Future* **2** 473–95

Ishidoya S, Sugawara H, Terao Y, Kaneyasu N, Aoki N, Tsuboi K and Kondo H 2020 O_2:CO_2 exchange ratio for net turbulent flux observed in an urban area of Tokyo, Japan and its application to an evaluation of anthropogenic CO_2 emissions *Atmos. Chem. Phys.* **20** 5293–308

Järvi L, Nordbo A, Junninen H, Riikonen A, Moilanen J, Nikinmaa E and Vesala T 2012 Seasonal and annual variation of carbon dioxide surface fluxes in Helsinki, Finland, in 2006–2010 *Atmos. Chem. Phys.* **12** 8475–89

Kent C W, Grimmond S, Barlow J, Gatey D, Kotthaus S, Lindberg, F and Halios C H 2017 Evaluation of urban local-scale aerodynamic parameters: implications for the vertical profile of wind speed and for source areas *Bound.-Layer Meteorol.* **164** 183–213

Kljun N, Calanca P, Rotach M and Schmid H 2004 A simple parameterisation for flux footprint predictions *Bound.-Layer Meteorol.* **112** 503–23

Kljun N, Calanca P, Rotach M and Schmid, H P 2015 A simple two-dimensional parameterisation for flux footprint prediction (FFP) *Geosci. Model Dev.* **8** 3695–713

Kunik L, Mallia D V, Gurney K R, Mendoza D L, Oda T and Lin J C 2019 Bayesian inverse estimation of urban CO_2 emissions: results from a synthetic data simulation over Salt Lake City, UT *Elementa* **7** 36

Lauvaux T *et al* 2016 High-resolution atmospheric inversion of urban CO_2 emissions during the dormant season of the Indianapolis Flux Experiment (INFLUX) *J. Geophys. Res.* **121** 5213–36

Lauvaux T *et al* 2020 Policy-relevant assessment of urban CO_2 emissions *Environ. Sci. Technol.* **54** 10237–45

Leclerc M Y and Foken T 2014 *Footprints in Micrometeorology and Ecology* (Berlin: Springer)

Lee T and Koski C 2014 Mitigating global warming in global cities: comparing participation and climate change policies of C40 cities *J. Comp. Policy Anal.: Res. Pract.* **16** 475–92

Lee X, Massman W and Law, B 2004 *Handbook of Micrometeorology: A Guide for Surface Flux Measurement and Analysis* (Dordrecht: Springer Science & Business Media)

Levin I and Karstens U 2007 Inferring high-resolution fossil fuel CO_2 records at continental sites from combined $^{14}CO_2$ and CO observations *Tellus* B **59** 245–50

Lietzke B, Vogt R, Feigenwinter C and Parlow E 2015 On the controlling factors for the variability of carbon dioxide flux in a heterogeneous urban environment *Int. J. Climatol.* **35** 3921–41

Menzer O and McFadden J P 2017 Statistical partitioning of a three-year time series of direct urban net CO_2 flux measurements into biogenic and anthropogenic components *Atmos. Environ.* **170** 319–33

Miles N L *et al* 2017 Quantification of urban atmospheric boundary layer greenhouse gas dry mole fraction enhancements in the dormant season: results from the Indianapolis Flux Experiment (INFLUX) *Elementa* **5** 27

Miller J B *et al* 2012 Linking emissions of fossil fuel CO_2 and other anthropogenic trace gases using atmospheric $^{14}CO_2$ *J. Geophys. Res.* **117** D08302

Miller J B, Lehman S J, Verhulst K R, Miller C E, Duren R M, Yadav V, Newman S and Sloop C D 2020 Large and seasonally varying biospheric CO_2 fluxes in the Los Angeles megacity revealed by atmospheric radiocarbon *Proc. Natl Acad. Sci.* **117** 26681–87

Nemitz E, Hargreaves K J, McDonald A G, Dorsey J R and Fowler D 2002 Micrometeorological measurements of the urban heat budget and CO_2 emissions on a city scale *Environ. Sci. Technol.* **36** 3139–46

Oda T *et al* 2019 Errors and uncertainties in a gridded carbon dioxide emissions inventory *Mitig. Adapt. Strateg. Glob. Change* **24** 1007–50

Olivier J and Janssens-Maenhout G 2012 CO_2 emissions from fuel combustion *IEA CO_2 Report*

Park C and Schade G W 2016 Anthropogenic and biogenic features of long-term measured CO_2 flux in north downtown Houston, Texas *J. Environ. Qual.* **45** 253–65

Prairie Y T and Duarte C M 2007 Direct and indirect metabolic CO_2 release by humanity *Biogeosciences* **4** 215–7

Reinmann A B, Smith I A, Thompson J R and Hutyra L R 2020 Urbanization and fragmentation mediate temperate forest carbon cycle response to climate *Environ. Res. Lett.* **15** 114036

Richardson S J *et al* 2017 Tower measurement network of *in-situ* CO_2, CH_4 and CO in support of the Indianapolis Flux (INFLUX) experiment *Elementa* **5** 59

Sargent M *et al* 2018 Anthropogenic and biogenic CO_2 fluxes in the Boston urban region *Proc. Natl Acad. Sci.* **115** 7491–6

Silva S J, Arellano A F and Worden H M 2013 Toward anthropogenic combustion emission constraints from space-based analysis of urban CO_2/CO sensitivity *Geophys. Res. Lett.* **40** 4971–6

Staufer J *et al* 2016 The first 1-year-long estimate of the Paris region fossil fuel CO_2 emissions based on atmospheric inversion *Atmos. Chem. Phys.* **16** 14703–26

Stull R B 2012 *An Introduction to Boundary Layer Meteorology* (Dordrecht: Springer Science & Business Media)

Sugawara H, Ishidoya S, Terao Y, Takane Y, Kikegawa Y and Nakajima K 2021 Anthropogenic CO_2 emissions changes in an urban area of Tokyo, Japan, due to the COVID-19 pandemic: a case study during the state of emergency in April–May 2020 *Geophys. Res. Lett.* **48** e2021GL092600

Turnbull J *et al* 2011 Assessment of fossil fuel carbon dioxide and other anthropogenic trace gas emissions from airborne measurements over Sacramento, California in spring 2009 *Atmos. Chem. Phys.* **11** 705–21

Turnbull J *et al* 2015 Toward quantification and source sector identification of fossil fuel CO_2 emissions from an urban area: results from the INFLUX experiment *J. Geophys. Res.* **120** 292–312

Turnbull J *et al* 2018 Synthesis of urban CO_2 emission estimates from multiple methods from the Indianapolis Flux Project (INFLUX) *Environ. Sci. Technol.* **53** 287–95

Turner A J, Shusterman A A, McDonald B C, Teige V, Harley R A and Cohen R C 2016 Network design for quantifying urban CO_2 emissions: assessing trade-offs between precision and network density *Atmos. Chem. Phys.* **16** 13465–75

Velasco E and Roth M 2010 Cities as net sources of CO_2: review of atmospheric CO_2 exchange in urban environments measured by eddy covariance technique *Geogr. Compass* **4** 1238–59

Vickers D and Mahrt L 1997 Quality control and flux sampling problems for tower and aircraft data *J. Atmos. Ocean. Technol.* **14** 512–26

Vogel F, Hamme S, Steinhof A, Kromer B and Levin I 2010 Implication of weekly and diurnal ^{14}C calibration on hourly estimates of CO-based fossil fuel CO_2 at a moderately polluted site in southwestern Germany *Tellus* B **62** 512–20

Vogt R, Christen A, Rotach M, Roth M and Satyanarayana A 2006 Temporal dynamics of CO_2 fluxes and profiles over a Central European city *Theor. Appl. Climatol.* **84** 117–26

Weng Q, Hu X, Quattrochi D A and Liu H 2013 Assessing intra-urban surface energy fluxes using remotely sensed aster imagery and routine meteorological data: a case study in Indianapolis, USA *IEEE J. Sel. Topics Appl. Earth Obs. Remote Sens.* **7** 4046–57

Wu D, Lin J C, Duarte H F, Yadav V, Parazoo N C, Oda T and Kort E A 2021 A model for urban biogenic CO_2 fluxes: solar-induced fluorescence for modeling urban biogenic fluxes (SMUrF v1) *Geosci. Model Dev.* **14** 3633–61

Wu K, Lauvaux T, Davis K J, Deng A, Coto I L, Gurney K R and Patarasuk R 2018 Joint inverse estimation of fossil fuel and biogenic CO_2 fluxes in an urban environment: an observing system simulation experiment to assess the impact of multiple uncertainties *Elementa* **6** 17